ELSEVIER

Physica A 236 (1997) 58–74

PHYSICA A

# Kinetics of conformational transitions of a single polymer chain

K.A. Dawson, E.G. Timoshenko*, Yu.A. Kuznetsov

*Theory Group, Centre for Soft Condensed Matter and Biomaterials, Department of Chemistry, University College Dublin, Dublin 4, Ireland*

**Abstract**

We seek to provide a general strategy to permit the study of non-equilibrium aspects of conformational transitions in various types of heteropolymers. The theoretical methods we have developed rely mainly on the Gaussian self-consistent approach that replaces the exact nonlinear Langevin equation by a linear stochastic ensemble with unknown time-dependent parameters determined in a self-consistent way. We discuss possible applications of the method to conformational transitions of biopolymers such as DNA and protein folding.

*PACS*: 36.20.-r; 64.70.Pf; 87.15.He; 87.15.-v
*Keywords*: Kinetics; DNA; Heteropolymer; Protein folding

## 1. Introduction

There are numerous problems involving dynamics and kinetics of conformational transitions of polymers that are of considerable scientific interest [1–4]. However, the lack of good general methods to study non-equilibrium problems of this type has been a limitation. This is a considerable contrast to the case of non-equilibrium statistical mechanics where the order parameter is related to a density [5]. In our case not only the density, but the fractal dimension may also change with time. Whilst computer simulation is undoubtedly quite successful in this arena [6, 7] it is important to be able to understand and interpret the results. For this reason we have taken steps to write down a general approach to the study of non-equilibrium phenomena where the fractal dimension may change. The general philosophy of our treatment is that, given the intractability of the full Langevin equation for the polymer, we should attempt to replace the exact equation with another "trial" dynamics which is exactly solvable. If we keep sufficient flexibility in this trial dynamics then all of the adjustable parameters

* Corresponding author. E-mail: timosh@fiachra.ucd.ie


*PII* S0378-4371(96)00396-2

may be varied to ensure that the trial and exact dynamics match each other as well as possible.

Finally, let us point out that apart from the intrinsic interest in the heteropolymer problem there has long been an underlying belief that such studies would lead us closer to an understanding of the phenomena of biopolymer folding or compaction as observed in proteins, DNA and other molecules. It is widely accepted that amongst the essential features required in a biopolymer model is the presence of "frustration" due to a combination of monomer units with some type of opposing tendency to associate or repel each other, along with some connectivity constraint.

## 2. Method

The phenomena we study are well described by the Langevin equation

$$\dot{x}_n^{\alpha}(t) = \sum_{\alpha',n'} \mathscr{H}_{nn'}^{\alpha\alpha'}[x(t)]\left(-\frac{\partial H}{\partial x_{n'}^{\alpha'}} + \eta_{n'}^{\alpha'}(t)\right). \tag{1}$$

Hydrodynamic effects are incorporated via $\mathscr{H}_{nn'}^{\alpha\alpha'}$, the Oseen hydrodynamic interaction tensor. The noise is assumed to have zero mean value and a second-order correlation function of the form

$$\langle \eta_n^{\alpha}(t)\,\eta_{n'}^{\alpha'}(t')\rangle = (\mathscr{H}^{-1})_{nn'}^{\alpha\alpha'}\,2k_BT\,\delta(t-t')\,. \tag{2}$$

The Hamiltonian $H = H_0 + H_{excl.v.}$ includes the spring and bending terms

$$H_0 = \frac{\kappa}{2}\sum_n (\boldsymbol{x}_n - \boldsymbol{x}_{n-1})^2 + \frac{k_BT\,\lambda}{2\,l^3}\sum_m (\boldsymbol{x}_{m+1} + \boldsymbol{x}_{m-1} - 2\boldsymbol{x}_m)^2\,, \tag{3}$$

where summation is performed only over the beads connected by springs with spring constant $\kappa = 3k_BT/l^2$, $l$ being the bond length and $\lambda/l$ the stiffness parameter [1,8,9]. The interaction part, $H_{excl.v}$, we present in the form of the virial expansion

$$H_{excl.v.} = \sum_{N=2}^{\infty} H_N = \sum_{N=2}^{\infty} u_N \sum_{m_1 \ldots m_N} \prod_{i=1}^{N-1} \delta(\boldsymbol{x}_{m_1} - \boldsymbol{x}_{m_{i+1}})\,, \tag{4}$$

where $u_N$ are virial coefficients and $m_1 \neq m_{i+1}$.

The present approach involves introduction of a time-dependent effective potential via the Gaussian stochastic ensemble for the Fourier modes,

$$\zeta_q(t)\dot{x}_q^{\alpha}(t) = -\Delta V_q(t)x_q^{\alpha} + \eta_q^{\alpha}(t)\,, \tag{5}$$

$$\langle \eta_q^{\alpha}(t)\,\eta_{q'}^{\alpha'}(t')\rangle = \zeta_q(t)\,2k_BT\,\delta(t-t')\delta_{\alpha\alpha'}\delta_{-qq'}\,. \tag{6}$$

Here, $\Delta V_q(t)$ and $\zeta_q(t)$ are, respectively, a time-dependent potential and friction that can be determined self-consistently.

The equations we give can then be used to follow the progress of the observables as the system passes to its new conformational state. Our main objects of study are the correlation functions,

$$\mathscr{F}_q(t) = \tfrac{1}{3}\langle |\boldsymbol{x}_q(t)|^2\rangle, \quad \mathscr{G}_q(t) = \tfrac{1}{3}\langle \boldsymbol{x}_{-q}(0)\boldsymbol{x}_q(t)\rangle\,. \tag{7}$$

We assume space-isotropic initial conditions and consequently all spatial components give equal contributions. Note that the squared radius of gyration is simply $R_g^2 = \sum_{q\neq 0}\mathscr{F}_q$. In terms of the time-dependent potential one can find the non-equilibrium equations of motion [10],

$$\frac{\zeta_q(t)}{2}\dot{\mathscr{F}}_q(t) = k_BT - \Delta V_q(t)\mathscr{F}_q(t)\,, \tag{8}$$

$$\zeta_q(t)\dot{\mathscr{G}}_q(t) = -\Delta V_q(t)\mathscr{G}_q(t)\,. \tag{9}$$

Let us introduce the following coefficients:

$$c^{(q)}_{nn'} = f^{(q)}_n - f^{(q)}_{n'}, \quad d^{(q)}_{nn',mm'} = \mathrm{Re}\, c^{(q)}_{nn'}\, c^{(-q)}_{mm'} \tag{10}$$

and the correlation functions

$$D_{nn',mm'} = \tfrac{1}{3}\langle(\boldsymbol{x}_n - \boldsymbol{x}_{n'})(\boldsymbol{x}_m - \boldsymbol{x}_{m'})\rangle = \sum_q d^{(q)}_{nn',mm'}\,\mathscr{F}_q\,. \tag{11}$$

Here $f^{(q)}_n = \exp(i2\pi qn/N)$ are the coefficients of the Fourier transform of a ring polymer. We shall also use the standard conventions [11] for reduction of the four-index coefficients to the two-index ones. Without hydrodynamics $\zeta_q \equiv \zeta = N\zeta_b$ is simply a constant. The self-consistent potential is related to the equal time correlation function by the following equation:

$$\Delta V_q\mathscr{F}_q = k_q\mathscr{F}_q + \frac{1}{3}\left\langle \boldsymbol{x}_{-q}(t)\frac{\partial H_{excl.v.}}{\partial \boldsymbol{x}_{-q}(t)}\right\rangle. \tag{12}$$

The effective potential may be written [11] as the derivative of the ensemble mean energy $\mathscr{E} = \langle H\rangle$,

$$\Delta V_q(t) = \frac{2}{3}\frac{\partial\mathscr{E}(t)}{\partial\mathscr{F}_q(t)}\,. \tag{13}$$

Now, recalling the expression for the entropy $\mathscr{S}$ in the Gibbs–Bogoliubov estimate at equilibrium,

$$\mathscr{S} = \frac{3}{2}k_B\sum_q \log\mathscr{F}_q\,, \tag{14}$$

one may rewrite Eq. (8) via the derivatives of the "instantaneous" free energy $\mathscr{A}(t) = \mathscr{E} - T\mathscr{S}$. For this, let us first introduce the real positive variable $X_q$ defined as the square root of the positive-definite quantity,

$$\mathscr{F}_q(t) = \tfrac{1}{3}X_q^2\,. \tag{15}$$

It is also instructive to use the $N$-dimensional vector notation $\boldsymbol{X} \equiv \{X_q\}$, and introduce the diagonal friction matrix $\zeta_{qq'} = \zeta_q \delta_{qq'}$. Then we shall have

$$\zeta \cdot \frac{d}{dt}\boldsymbol{X}(t) = -\frac{\partial \mathscr{A}(t)}{\partial \boldsymbol{X}(t)}, \tag{16}$$

where the dot designates the scalar product.

The form in Eq. (16) is useful for understanding the kinetics of a homopolymer as the evolution in the phase space of the dynamical variables $\boldsymbol{X}$ against the gradient of the free energy, i.e. in the direction of its deepest descent. Thus, at equilibrium the system is in the absolute minimum. After the quench it happens to be at a non-stationary point and starts moving towards the new absolute minimum of the free energy.

The rate of kinetics could be described by the time derivative of the free energy as well as the modulus of its gradient. Indeed, it is simple to calculate the time derivative of the free energy from Eq. (16):

$$\frac{d}{dt}\mathscr{A}(t) = -\frac{\partial \mathscr{A}}{\partial \boldsymbol{X}} \cdot \zeta^{-1} \cdot \frac{\partial \mathscr{A}}{\partial \boldsymbol{X}}. \tag{17}$$

The ensemble averaged energy is given by [10]

$$\mathscr{E} = \frac{3\,k_B TN}{2\,l^2} \sum_q d_{01}^{(q)} \left(1 + \frac{\lambda}{l} d_{01}^{(q)}\right) \mathscr{F}_q + \sum_{L=2}^{\infty} \hat{u}_L \sum_{m_1 \ldots m_L} (\det \Delta^{(L-1)})^{-3/2}. \tag{18}$$

In this formula $\Delta^{(L-1)}$ is a matrix of the size $L-1$ with the matrix elements

$$\Delta_{ij}^{(L-1)} = D_{m_1 m_{i+1}, m_1 m_{j+1}} \tag{19}$$

and $\hat{u}_L = u_L/(2\pi)^{3(L-1)/2}$.

## 3. Flexible homopolymer

We found [10–12] that for a flexible homopolymer there are four characteristic stages in the kinetics from the Flory coil to the conventional collapsed state. The stages are as follows:

(a) At early stages we find a sort of spinodal decomposition where many of the internal modes of the polymer coil become unstable. Initially, the chain undergoes formation of small locally collapsed globules that grow for some time at the expense of their neighbours in the chain. This process leads to an essential decrease of amplitudes of large-$q$ modes, these describing the local structure of the chain. There is also a much slower decrease of low-$q$ modes, describing the polymer at large distances along the chain. The squared radius of gyration first decreases according to the power law [10]

$$R_g^2(t) = R_g^2(0) - A_1 t^{\alpha_i}, \tag{20}$$

where $\alpha_i = \frac{7}{11}$ ($\alpha_i = \frac{9}{11}$) without (with) hydrodynamic interaction. At the end of this stage most of the slack polymer has been gathered up into small more condensed

clusters with relatively tight chain between them. The effective Flory exponent has risen to be unity, characterizing a rigid rod of clusters, and thereafter begins to fall rapidly until it reaches a near-ideal Gaussian value.

(b) The second stage involves cluster coarsening, the analogue of Lifshitz–Slyozov cluster growth after a quench into the liquid–gas coexistence region. However, we emphasize that this chain of clusters is essentially an ideal coil at long lengths with a set of topologically connected locally collapsed clusters. The evidence is that the average effective swelling exponent during this stage corresponds to an ideal coil $\nu_T = \frac{1}{2}$, and we therefore have a set of clusters growing against the tension of an ideal coil elasticity. The characteristic time expected from elementary arguments is

$$\tau_m = AN^{2\beta_T} \quad (\tau_m = A'N^{3\nu_T}) \tag{21}$$

for the model without (with) hydrodynamic interaction. Thus, we get the cluster growth law without hydrodynamics,

$$S(t) = A_s t^Z, \quad Z = \tfrac{1}{2}. \tag{22}$$

The latter prediction is in agreement with the result obtained by de Gennes in his seminal work on the collapse kinetics [13]. These are then the fundamental laws of collapse throughout the predominant stage of kinetics, for beyond this stage the polymer coil is space-filling, though not yet compacted.

(c) The next stage corresponds to shape optimization and further compaction of the globule to a higher density. Here the mean squared radius of gyration tends exponentially slowly to the final equilibrium value,

$$R_g^2(t) = R_g^2(\infty) + A_f \exp(-t/\tau_f). \tag{23}$$

The relaxation time scales in the degree of polymerization $\tau_f \sim N^{\gamma_f}$ in the following way [11]: $\gamma_f = 2\nu_c + 1$ ($\gamma_f = 3\nu_c$) without (with) hydrodynamics, where $\nu_c = \frac{1}{3}$ is the collapsed swelling exponent.

(d) Due to topological restrictions the late state of kinetics for a non-phantom chain will have a different structure than for a phantom one. For an open polymer topological restrictions may be removed via self-reptations of the chain, and it has been argued that this leads to an even longer final kinetic stage with the time scale $\tau_{\text{reptations}} \sim N^3$ [14].

## 4. Stiff homopolymer

Our initial probes of the model [15] revealed a sort of slowing-down in kinetics of a stiff chain in agreement with Ref. [16]. In that work the model of the freely rotating chain has been adopted for studying the contraction kinetics of a moderatively stiff and relatively *thick* chain. It was noted that the slowing-down is related to the higher degree of cooperativity required for a rigid chain to rearrange itself during contraction. Although this is partially true, no explicit mechanism of this phenomenon has been given. It is also unclear whether the observed effect occurred due to the stiffness or

really due to the thickness, phenomenologically described by the two-body screened interaction term.

Naturally, it was interesting to check whether the same behavior is reproduced in the present model of rigidity. We have checked that and found a quite similar picture for the given parameters of the Hamiltonian. Quite surprisingly though, the effect has completely disappeared for the same stiffness by switching off the thickness parameter. Only for rather higher stiffness it was possible again to recover a sort of the slowing-down.

In addition, we should note here that we have earlier observed such kinetic phenomenon in our study of copolymers [17] and only now are the connections becoming clear to us. Further surprises consisted in that it was possible for the same rigidity to produce one, two or no slow regimes in kinetics by changing the quench depth. By studying the heat capacity, bending energy and the correlations of monomer positions along the chain, $D_m$, it has become evident to us that for high rigidity parameter the system may undergo a transition to a new toroidal phase, and also that the kinetics depends crucially on how close one is to the spinodals associated with first-order transitions.

There is a significant amount of theoretical [18] and experimental [19] literature dealing with various questions about equilibrium properties of rigid chains, the most important practical example of which is DNA. Experimentally, it is well known that DNA can acquire a torus-like shape in its globular state, and that condensation of DNA induced by various agents could lead to even more complicated phases [19]. In theory the torus shape has been predicted in Ref. [20]. The physical reason for a torus is clear – a persistent chain has no desire to bend, so it tends to have as large a radius of curvature as possible, consistent with quite close packing of the chain. Nevertheless, to construct a good qualitative theory of such states is not very simple [18].

In Fig. 1 we present the phase diagram of the model in variables of the stiffness, $\lambda$, and the second virial coefficient, $u_2$. The coil phase corresponds to extended conformations of the polymer with a large radius of gyration scaling as $R_g \sim N^{\nu_{coil}}$, where the exponent $\nu_{coil}$ is close to the Flory value $\nu_F = \frac{3}{5}$ for a flexible chain, becomes a rigid rod exponent $\nu_{rod} = 1$ for a very stiff chain, with a cross-over in between. A new feature here, in comparison to the case of a flexible homopolymer, is that there are two compact states of the system: the spherical globule, which is just a conventional globule, and the torus-like globule.

Curve I in Fig. 1 denotes the ordinary coil-to-globule transition for a comparatively flexible chain. This is a continuous (second-order) transition. If the stiffness is greater than some critical value the collapse transition (curve II in Fig. 1) becomes discontinuous (first-order transition). The discontinuity of the coil-to-torus transition is natural since it is accompanied by a change in the spatial symmetry. It turns out that for larger $|u_2|$ the system can undergo a torus-to-spherical globule discontinuous transition (curve III in Fig. 1) restoring the spatial isotropy of the globule. Note that all curves I–III intersect at a bicritical point A. Evidently, the transition III occurs when the two-body attraction exceeds the bending elasticity contribution.

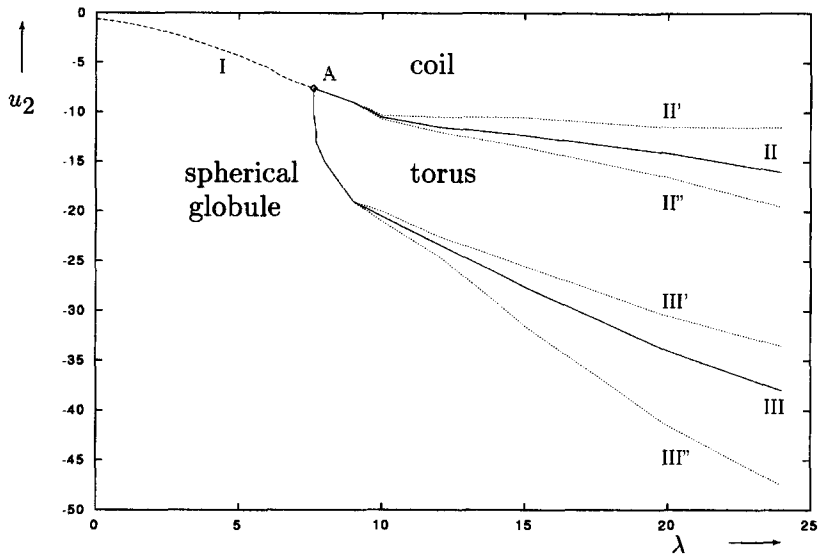


Fig. 1. The phase diagram of a stiff homopolymer in variables of the stiffness parameter $\lambda$ and the second virial coefficient $u_2$. Curve I corresponds to the second-order phase transition and curves II, III to the first-order transitions. Point A is a bicritical point. Curves II', II" and III', III" are spinodals. This diagram has been obtained from the data for polymer with the degree of polymerization $N = 100$.

Let us consider now the kinetics for a similar quench at a relatively small stiffness $\lambda < \lambda_c$, where the equilibrium collapse transition (curve I in Fig. 1) is still second-order. The kinetics remains qualitatively the same, but it takes longer and the spinodal decomposition effect becomes weaker with increasing stiffness. The time-scale of the middle stage $\tau_m$ may be estimated as

$$\tau_m(\lambda) \sim \tau_m^{flex} + a\,\lambda^{1.2\pm0.1}\,N^{1.3\pm0.2}\,. \tag{24}$$

Since the kinetics in Eq. (16) is simply the motion against the free energy gradient, in Fig. 2 we schematically illustrate the free energy profiles for different values of $u_2$. Let us emphasize here that the torus minimum lies farther from the initial coil minimum than the spherical globule one. To explain this property one may argue that the spherical globule minimum may be obtained by a continuous deformation of the coil minimum, what corresponds to the second-order of the coil-to-spherical globule transition (curve I in the phase diagram), whereas the torus is a topologically different conformation and may be obtained from the coil by a first-order transition (curve II).

Thus, we start at the point A in Fig. 2, which is the unique free energy minimum for the coil. After an instantaneous quench the initial profile is transformed and the system happens to be in a point along the arrow A–E. The resulting kinetics depends on the free energy profile for appropriate final value of $u_2$.

The situation changes dramatically after the bicritical point $\lambda_c$. In Fig. 3 the time evolution of the mean energy for quenches with different final second virial coefficients

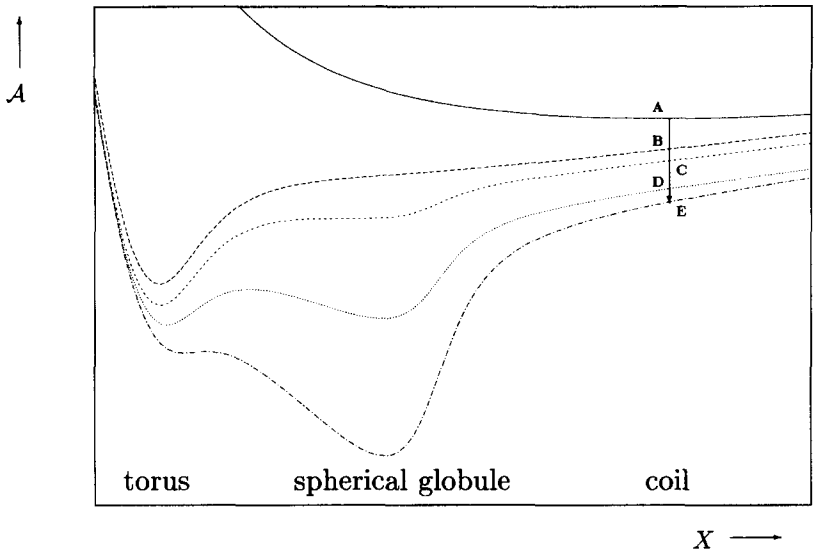


Fig. 2. Schematical profiles of the free energy $\mathscr{A}$ parametrized by the dynamical variables $X$ for different values of the second virial coefficient $u_2$. The system is quenched from the point A (which corresponds to the global free energy minimum for the extended coil) along the arrow to points: B (quench to the torus state), C (the same with a kinetic slowing down), D (quench to the metastable spherical globule state), and E (quench to the stable spherical globule state).

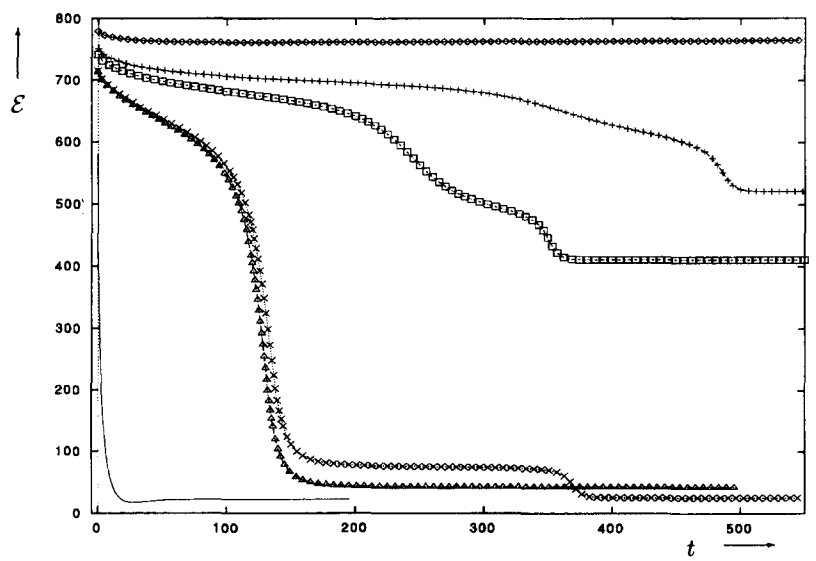


Fig. 3. Time evolution of the mean energy $\mathscr{E}$ for $N = 100$, $\lambda = 15$ for different quenches from the coil state $u_2^i = 15$ (from top to bottom): (diamonds) $u_2 = -12$ (quench inside the coil state), (pluses) $u_2 = -18$ (quench to the torus state just beyond the spinodal II"), (quadrangles) $u_2 = -20$ (quench deep to the torus state), (crosses) $u_2 = -25.6$ (quench to the torus state just above the spinodal III') and (triangles) $u_2 = -26$ (quench to the metastable region between the curves III' and III"). Here the solid line is drawn rescaled: $500 + \mathscr{E}/2$ for convenience.

are depicted. One observation is that the kinetics of a stiff polymer is considerably longer than of a flexible polymer (solid curve). Another observation from Fig. 3 is that the kinetic process has several slow and fast regimes. Their duration and even number depends strongly on the quench depth.

The characteristic kinetic time on approaching a spinodal line from within the stable region diverges as a power law

$$\tau \sim |u_2 - u_2^s|^{-\delta^s}, \tag{25}$$

and kinetics is trapped once one has entered a metastable region. We have extracted the following critical exponents: $\delta^{II''}_{-} = \frac{3}{2}$, $\delta^{III'_{+}} = \delta^{III''}_{-} = \frac{1}{2}$) describing the slowing down near different spinodal lines in Fig. 1 that separate regions of metastability.

## 5. Random copolymer

For the sequence model [21–23] the interaction potential $H = \bar{H} + \tilde{H}$ consists of the homopolymeric $\bar{H}$ and the disordered $\tilde{H}$ parts respectively,

$$\bar{H} = \frac{K}{2}\sum_{n}(\boldsymbol{x}_{n+1} - \boldsymbol{x}_n)^2 + \sum_{L>2}\bar{u}_L \sum_{\{m\}}\prod_{i=1}^{L-1}\delta(\boldsymbol{x}_{m_i} - \boldsymbol{x}_{m_{i+1}}), \tag{26}$$

$$\tilde{H} = \frac{1}{2}\sum_{m_1 m_2}(\Lambda_{m_1} + \Lambda_{m_2})\delta(\boldsymbol{x}_{m_1} - \boldsymbol{x}_{m_2}), \tag{27}$$

where $\Lambda_m$ are independent random variables on a half-period with the Gaussian distribution of disorder,

$$P(\{\Lambda\}) = \prod_m \frac{1}{(2\pi\Delta^2)^{1/2}} \exp\left(-\frac{\Lambda_m^2}{2\Delta^2}\right). \tag{28}$$

The Fourier transforms $\{\lambda\}$ are also independent random Gaussian variables with zero mean value and dispersion $\bar{\Delta}^2$,

$$\overline{\lambda_q \lambda_{q'}} = \bar{\Delta}^2 \delta_{q+q',0}, \quad \bar{\Delta}^2 \equiv \Delta^2/N. \tag{29}$$

Henceforth, we use the brackets $\langle A\rangle$ to denote the statistical averages over the noise and initial ensemble of monomer positions $\{\boldsymbol{x}(t=0)\}$ and the bar $\bar{A}$ to denote averages over the quenched distribution of disorder $\{\Lambda\}$.

Apart from the observable $\mathscr{F}_q = \overline{\langle|\boldsymbol{x}|_q^2\rangle}$ this system requires for its description the additional variable defined by

$$\varphi_{qp}(t) \equiv \overline{\phi_{qp}(t)}, \quad \phi_{qp}(t) = \tfrac{1}{3}\lambda_{q-p}\langle \boldsymbol{x}_{-q}(t)\boldsymbol{x}_p(t)\rangle. \tag{30}$$

The kinetic equations for this model may be written in terms of the derivatives of the free energy $\mathscr{A}$ with respect to the dynamical variables as follows [24]:

$$\frac{\zeta}{2}\frac{d}{dt}\mathscr{F}_q(t) = -\frac{2}{3}\left(\mathscr{F}_q\frac{\partial\mathscr{A}}{\partial\mathscr{F}_q} + \sum_p \varphi_{qp}\frac{\partial\mathscr{A}}{\partial\varphi_{qp}}\right), \tag{31}$$

$$\zeta\frac{d}{dt}\varphi_{qp}(t) = -\frac{2}{3}\left(\varphi_{qp}\left(\frac{\partial\mathscr{A}}{\partial\mathscr{F}_q} + \frac{\partial\mathscr{A}}{\partial\mathscr{F}_p}\right) + \bar{\Delta}^2(\mathscr{F}_q + \mathscr{F}_p)\frac{\partial\mathscr{A}}{\partial\varphi_{qp}}\right). \tag{32}$$

This form of the kinetic equations has a transparent meaning. Indeed, the folding kinetics could be understood as a motion on the surface of the free energy parametrized by dynamical variables $\mathscr{F}_q$, $\varphi_{qp}$. The motion is determined by gradients and is directed towards the global energy minimum. Here the free energy landscape determining the kinetics represents the flow of the whole statistical ensemble.

The free energy $\mathscr{A}[V_q, U_{qp}] = \mathscr{E} - T\mathscr{S}$ contains the "entropic" part

$$\mathscr{S} = k_B\frac{3}{2}\sum_q \log\mathscr{F}_q - k_B\frac{3\bar{\Delta}^{-2}}{4}\sum_{qp}\frac{\varphi_{qp}^2}{\mathscr{F}_q\mathscr{F}_p} + \mathrm{O}(\bar{\Delta}^4), \tag{33}$$

and the mean energy $\mathscr{E} = \overline{\langle H\rangle}$,

$$\begin{aligned}\frac{\overline{\langle H\rangle}}{N} = {} & \frac{3\kappa}{2}\mathscr{D}_{01} + \hat{u}_2\sum_k\frac{1}{\mathscr{D}_k^{3/2}} + \hat{u}_3\sum_{k_1k_2}\frac{1}{Y_0(k_1,k_2)^{3/2}} \\ & - \frac{3}{2}\hat{1}\sum_k\frac{\Phi_k}{\mathscr{D}_k^{5/2}} + \hat{u}_2\frac{15}{8}\sum_k\frac{P_{k,k}}{\mathscr{D}_k^{7/2}} \\ & + \hat{u}_3\frac{15}{8}\sum_{k_1k_2}\frac{Y_2(k_1,k_2)}{Y_0(k_1,k_2)^{7/2}} - \hat{u}_3\frac{3}{2}\sum_{k_1k_2}\frac{Y_3(k_1,k_2)}{Y_0(k_1,k_2)^{5/2}}\,.\end{aligned} \tag{34}$$

Here we have used the following set of definitions:

$$Y_0(k_1,k_2) = \mathscr{D}_{k_1}\mathscr{D}_{k_2} - \mathscr{D}_{k_1k_2}^2, \tag{35}$$

$$\begin{aligned}Y_2(k_1,k_2) = {} & \mathscr{D}_{k_1}^2 P_{k_2,k_2} + \mathscr{D}_{k_2}^2 P_{k_1,k_1} + 4\mathscr{D}_{k_1k_2}^2 P_{k_1k_2,k_1k_2} \\ & + 2\mathscr{D}_{k_1}\mathscr{D}_{k_2}P_{k_1,k_2} - 4\mathscr{D}_{k_1k_2}(\mathscr{D}_{k_2}P_{k_1,k_1k_2} + \mathscr{D}_{k_1}P_{k_2,k_1k_2})\end{aligned} \tag{36}$$

$$Y_3(k_1,k_2) = P_{k_1,k_2} - P_{k_1k_2,k_1k_2}\,, \tag{37}$$

$$\Phi_k = \sum_{q,p} d_k^{(q,p)}\varphi_{q,p}\,.$$

We have also denoted

$$P_k^{(s)} = \sum_p d_k^{(p,\,p+s)}\,\varphi_{p,\,p+s}\,, \tag{38}$$

$$P_{k_1,k_2} = \bar{\Delta}^{-2}\sum_s P_{k_1}^{(s)}P_{k_2}^{(s)} = \overline{D_{k_1}D_{k_2}}^{(c)} \tag{39}$$

with the coefficients

$$d_k^{(q,p)} = \tfrac{1}{2}(d_k^{(q)} + d_k^{(p)} - d_k^{(q-p)}) . \tag{40}$$

Two important order parameters in this model are the glass parameter, which is related to the sample to sample fluctuation of the squared radius of gyration [25],

$$\overline{R_g^2 R_g^2}^{(c)} = \bar{\Delta}^{-2} \Upsilon^2, \quad \Upsilon = \sum_{q \neq 0} \varphi_{qq} , \tag{41}$$

and the phase separation parameter,

$$\Psi = \frac{1}{6N^2} \sum_{mm'} \overline{(\Lambda_m + \Lambda_{m'} - 2\lambda_0) D_{mm'}} , \tag{42}$$

$$\Psi = \sum_{q \neq p, q, p \neq 0} \varphi_{qp} . \tag{43}$$

For just two types of monomers "A" and "B" with equal concentrations $n_A = n_B = \frac{1}{2}$ the latter reduces simply to $\Psi = \frac{1}{2}(R_g^2(B) - R_g^2(A))$.

In Fig. 4 we exhibit the time dependence of the phase separation order parameter $\Psi$ defined by Eq. (43) for different dispersions of disorder. This quantity is identically zero for a homopolymer and remains small for very weak disorder. For early times $\Psi(t)$ rapidly grows reaching its maximum near the end of the spinodal stage. This reflects the formation of micro-phase structure of growing clusters, which tend to have hydrophilic exterior and hydrophobic core. During most of the coarsening stage $\Psi$ changes only slightly. Indeed, the micro-domain structure of the coalescing globule has already been formed. It is represented by the original clusters, which essentially preserve their integrity within the macro-globule. If $\Delta$ is insufficiently large, the folding ends up after optimization of the relative positions of these subclusters and the surface area. However, for stronger disorder, $\Delta > \Delta_r$ (upper curve), at some moment around $\tau$ the system undergoes further and abrupt phase separation on larger scales. This phenomenon has an obvious similarity to that of the phase separation order parameter $Z$ in periodic heteropolymers (see Ref. [17]).

Now let us compare these observations with the behavior of the glass order parameter $\overline{R_g^2 R_g^2}^{(c)}$ presented in Fig. 5. The latter can behave in a rather diverse manner depending on the value of $\Delta$. We can distinguish at least four different regimes listed in order of increasing $\Delta$ and designated by the curves labelled below as in the figure:

(A) this quantity is almost zero during the first stage, then grows during the second, but after reaching the maximum falls down to zero;

(B), (C) similar to (A) first, but after reaching its maximum decreases slightly and remains at a high level, where it finally remains;

(D) the same as above, but after the critical dispersion $\Delta_r$ it falls rapidly to a level very close to zero. Comparing this with the previous figure, we find that the critical dispersion is, in fact, the same for glassy and phase separation order parameters.

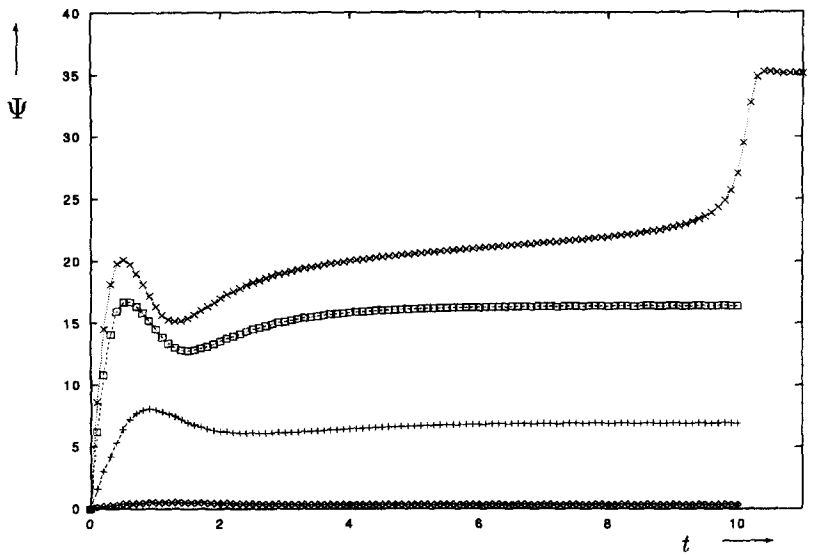


Fig. 4. Plots of the phase separation order parameter $\Psi$ versus time $t$ for different values of the dispersion of disorder (from bottom to top): $\Delta = 4, 16, 32, 38$. Here and in the next figure the values of the parameters are the following: the degree of polymerization $N = 40$, the third virial coefficient $\tilde{u}_3 = 10$, the initial and final second virial coefficient $\tilde{u}_2^{(i)} = 15$, $\tilde{u}_2^{(f)} = -25$, and the initial dispersion of disorder $\Delta^{(i)} = 0$.

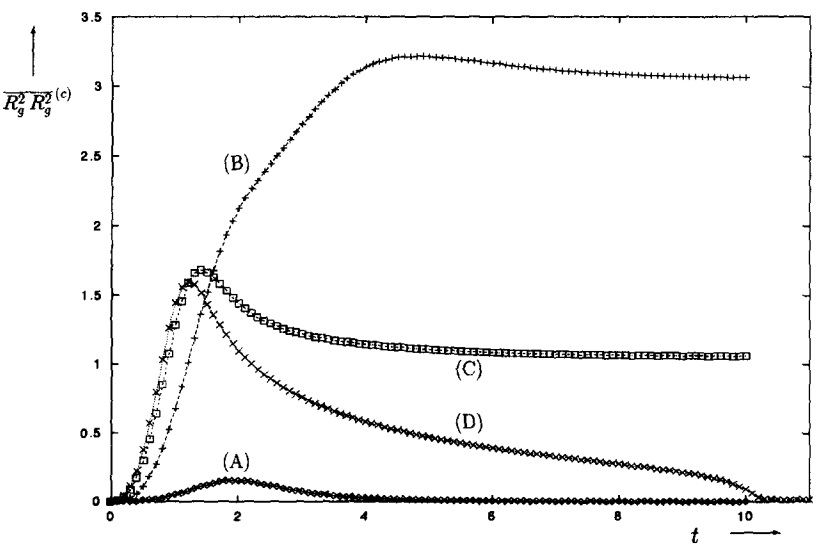


Fig. 5. Plots of the sample to sample fluctuation of the squared radius of gyration $\overline{R_g^2 R_g^2}^{(c)}$ versus time $t$. Lines (A)–(D) correspond, respectively, to the values of the dispersion of disorder $\Delta = 4, 16, 32, 38$.

Thus, to resume, the system is strongly frustrated during the coarsening stage and forms a sort of glass. The frustration is induced by the hydrophilic shells of the subclusters and by the polymeric bonds. Thus, the system is kinetically arrested and possesses, as we shall see below, a long relaxation time due to the height of potential barrier. Existence of such glassy structure is clearly manifested in the glass order parameter $\overline{R_g^2 R_g^2}^{(c)}$. Thus, Fig. 5 tells us that there are at least three different final phases of the system distinguished by the glass order parameter: for small $\Delta$ there is a liquid-like globule (LG), which is akin to an ordinary homopolymer globule with zero glass order parameter; glassy phase (G) with nonzero $\overline{R_g^2 R_g^2}^{(c)}$, and for $\Delta > \Delta_r$ there is a *folded* phase (F) characterized by (almost) vanishing glass order parameter and a large phase separation order parameter. It is clear that the glassiness is destroyed by the final larger-scale phase separation. The globule acquires a more organized internal structure and becomes more compact.

These observations are quite striking. In broad terms the states predicted here are close to those that have been discussed for real proteins [26].

The delay time near the transition line may be estimated with a good precision as a power law $\tau \simeq A(\Delta - \Delta_r)^{-\gamma}$. For quenches to the folded state but close to the renaturation transition line the delay time analogously to the stiff chain diverges as a power law with the exponent approximately equal to $\gamma = \frac{1}{2} \pm 0.04$. This delay time $\tau$ also grows with the degree of polymerization $N$ since the prefactor scales as $A \sim N^{5/3 \pm 0.12}$. Moreover, the critical dispersion of this transition $\Delta_r$ increases significantly with $N$.

Having discussed the kinetics of folding, let us turn our attention to the final state of kinetics, i.e. the equilibrium phase structure of the model. There we indeed observe the two-phase transitions discovered above. When the dispersion of disorder reaches the critical value $\Delta_f$, which scales as a positive power of $u_3$, the system undergoes the *freezing* transition accompanied by an abrupt increase of the glass order parameter. At this phase transition the phase separation order parameter changes quite regularly. In fact, $\Psi$ grows linearly until the second, *renaturation* transition, at $\Delta_r$, where it has a rapid jump, and then further grows linearly. Remarkably, the glass order parameter quickly drops to almost zero at the point $\Delta_r$.

The reason why we may conjecture this transition to be related to the renaturation becomes clear from Fig. 6. The homopolymer correlations of monomer positions (solid line), $\mathscr{D}_k$, satisfy the following scaling law: $\mathscr{D}_k \sim k$ for $|k| < N^{2/3}$ and $\mathscr{D}_k \sim N^{2/3}$ otherwise [11,27]. This law is preserved as one switches on the dispersion of disorder, and it is still fulfilled in the glassy phase (curve denoted by diamonds). Renaturation transition, however, leads to a striking modification of this law: $\mathscr{D}_k \sim const$ for any but very small $k$ (curve denoted by pluses). Thus, the correlations of monomer coordinates do not depend on their chain indices after we have integrated over all possible complexions of disorder. They are equal to a universal constant entirely determined by the excluded volume interaction structure.

Finally, let us discuss the mean squared radius of gyration $\overline{R_g^2}$ versus the dispersion $\Delta$ drawn in Fig. 7. Generally speaking, the size of the polymer is almost independent of $\Delta$ in the LG phase, becomes larger in the glassy phase and is much smaller in the

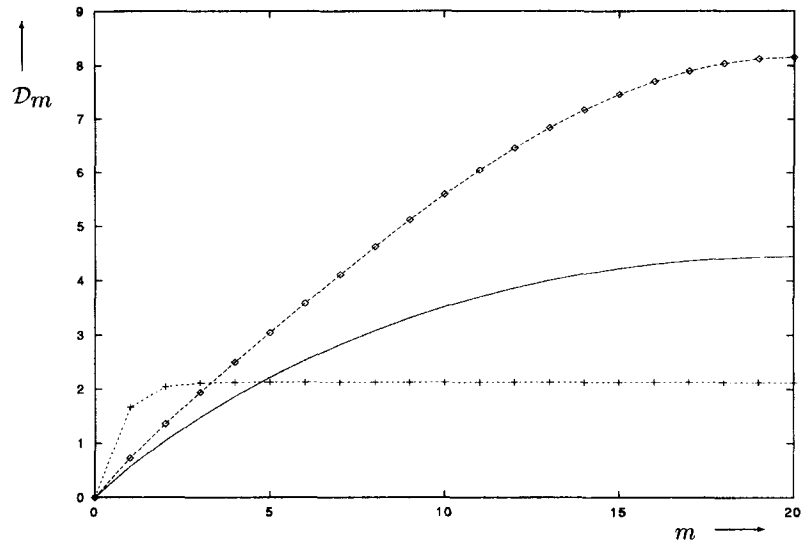


Fig. 6. Plots of the equilibrium correlations of monomer coordinates $\mathcal{D}_m$ versus the chain index $m$ for polymer with the degree of polymerization $N = 40$ and values of the second and the third virial coefficients $\tilde{u}_2 = -25$ and $\tilde{u}_3 = 10$: (solid line) $\Delta = 0$ (homopolymer), (diamonds) $\Delta = 16$ and (pluses) $\Delta = 38$.

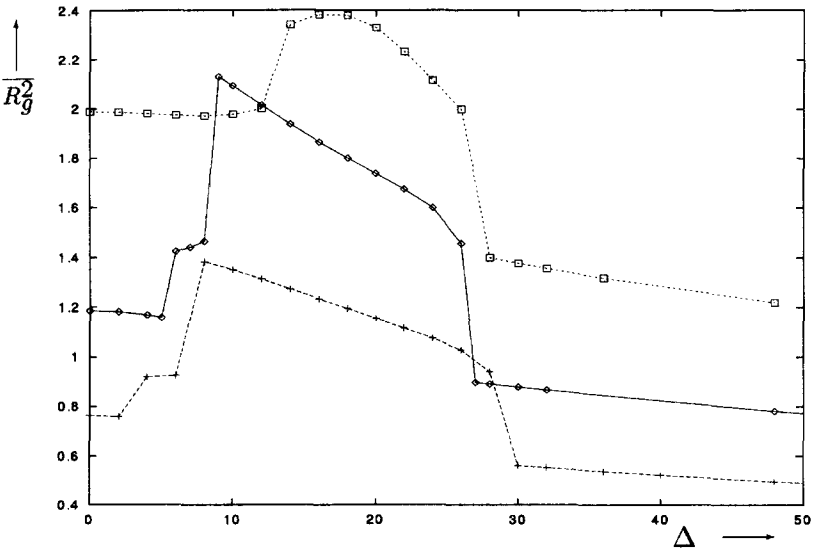


Fig. 7. Plots of the equilibrium mean squared radius of gyration $\overline{R_g^2}$ versus the dispersion of disorder $\Delta$ for different values of the third virial coefficient (from bottom to top): $\tilde{u}_3 = 5, 10, 20$. The degree of polymerization and the second virial coefficient are $N = 30$ and $\tilde{u}_2 = -25$.

F phase. Thus, the globule in the folded state is more compact than the homopolymer one and depends weakly on the dispersion of disorder. These properties conform to the intuitive idea that a glassy globule should be bigger since parts of the chain are frozen in not completely compacted locations, and that the native globule should be maximally compacted due to the best possible optimization of the volume interactions. In addition, the mean energy becomes smaller in the folded state as well.

## 6. Conclusions

We have spent some time discussing the details of the Gaussian self-consistent approximation for dealing with conformational kinetic phenomena. We believe that it has many potential advantages because it is well defined, simple to apply, and has a known limiting behavior at equilibrium. However, we will now discuss the problems that one can expect to face in application of our ideas. The most serious is already clear from a study of the equilibrium equations, a matter that has been discussed with clarity in Ref. [3], as well as various references therein. Thus, if we set the time derivatives to zero we obtain an equation for the effective potential. This equation is precisely what one would obtain using a Gaussian variational calculation, and it is known that for the case of an infinite repulsive potential we find a Flory exponent that has too large a value. Nevertheless, the qualitative features of collapse and other transitions are well preserved and with some reasonable assumptions, but without mathematical control, we can recover the Flory exponents [28]. The point that we seek to make here is that the relations between exponents are all preserved. Our experience of the non-equilibrium method is fairly favourable also. We believe that relations between various quantities are well preserved in the non-equilibrium method we have presented, and results from various simulation studies and comparisons to previous works have helped confirm this [29,10,30].

Of course, fundamentally we deal with a phantom network. We note that this is not the same as a phantom chain, and the fact that there are effective springs connected between all pairs has the effect of restraining crossing. In any case, the method has been applied to problems with known kinetic laws, and good agreement has been found. The effect of non-phantomness has been studied in Monte Carlo simulation for a homopolymer in Ref. [14]. It is quite important in the dense globular state. For an open polymer topological restrictions may be removed via self-reptations of the chain, and it has been argued that this leads to an even longer final kinetic stage with the time scale $\tau_{\text{reptations}} \sim N^3$. However, this is a delicate question that requires a separate study.

In general, therefore, we believe that the method gives very good qualitative and in some cases quantitative predictions. One should note that this assessment is based on our experience with a particular class of problems and the intuitions based on these so, in time, later applications may lead to some revision of these positive views. The final resolution to these questions must take a different direction. Thus, the Gaussian nature of the trial distribution is its weakest aspect, and the basic philosophy of our

approach may be expected to have broader application than with this particular choice. A better choice of distribution than the Gaussian appears to be possible. There is real promise now that one can write out a theory that has the correct equilibrium limits and accurate Flory exponents [30]. However, this promise bring with it also the unfortunate aspect that methods for kinetics that go much beyond what we have discussed here are difficult to analyze except by extensive numerical study. It will be challenging to see what can be done to improve the situation [30].

On the broader issues of what may be expected from non-equilibrium studies of differing types of polymers, copolymers, and biopolymers, some matters are becoming clearer. In particular, it does now seem likely that in due course a reasonably complete understanding of the fundamental kinetic laws of these systems can be acquired along the lines we have discussed. Whether we will be able to make the intellectual connection to these approaches remains an open, but important, question which should be resolved in the not too distant future.

## Acknowledgements

The authors acknowledge interesting discussions with Professors B. Chu, P.G. de Gennes, A.Yu. Grosberg, A.R. Khokhlov, P. Pincus, Y. Rabin, B. Widom, K. Yoshikawa, and our colleagues Dr. A. Gorelov and A. Moskalenko.

## References

[1] M. Doi and S.F. Edwards, The Theory of Polymer Dynamics (Oxford Science, New York, 1989).
[2] P.G. de Gennes, Scaling Concepts in Polymer Physics, 3rd printing (Cornell University Press, Ithaca, NY, 1988).
[3] J. des Cloizeaux and G. Jannink, Polymers in Solution (Clarendon Press, Oxford, 1990).
[4] B.H. Zimm, J. Chem. Phys. 24 (1956) 269; B.H. Zimm, G.M. Roe and L.F. Epstein, J. Chem. Phys. 37 (1962) 2547; H. Yamakawa, Modern Theory of Polymer Solutions (Harper & Row, New York, 1971); S.F. Edwards and K.F. Freed, J. Chem. Phys. 61 (1974) 1189; S.F. Edwards and M. Muthukumar, Macromolecules 17 (1984) 586; A.J. Peterlin, J. Chem. Phys. 23 (1955) 2464; Y. Oono and M. Kohmoto, J. Chem. Phys. 78 (1983) 520.
[5] S. Ma, Statistical Mechanics (World Scientific, Philadelphia, 1985).
[6] B. Ostrovsky and Y. Bar-Yam, Comput. Polym. Sci. 3 (1993) 9; M.A. Smith, Y. Bar-Yam, Y. Rabin, B. Ostrovski, C.A. Bennett, N. Margolus and T. Toffoli, Comput. Polymer Sci. 2 (1992) 165.
[7] A. Byrne, P. Kiernan, D. Green and K.A. Dawson, J. Chem. Phys. 102 (1995) 573.
[8] O. Kratky and G. Porod, Rec. Trav. Chim. 68 (1949) 1106; H. Yamakawa, Ann. Rev. Phys. Chem. 35 (1984) 23.
[9] R.A. Harris and J.E. Hearst, J. Chem. Phys. 44 (1966) 2595.
[10] E.G. Timoshenko, Yu.A. Kuznetsov and K.A. Dawson, J. Chem. Phys. 102 (1995) 1816.
[11] Yu.A. Kuznetsov, E.G. Timoshenko and K.A. Dawson, J. Chem. Phys. 104 (1996) 3338.
[12] Yu.A. Kuznetsov, E.G. Timoshenko and K.A. Dawson, J. Chem. Phys. 103 (1995) 4807.
[13] P.G. de Gennes, J. Phys. Lett. 46 (1985) L639.
[14] A.Yu. Grosberg and D.V. Kuznetsov, Macromolecules 26 (1993) 4249.
[15] Yu.A. Kuznetsov, E.G. Timoshenko and K.A. Dawson, J. Chem. Phys. 105 (1996) 7116.
[16] F. Ganazzoli, R. La Ferla and G. Allegra, Macromolecules 28 (1995) 5285.
[17] E.G. Timoshenko, Yu.A. Kuznetsov and K.A. Dawson, Phys. Rev. E 53 (1996) 3886.

[18] V.A. Bloomfield, Biopolymers 31 (1991) 1471; J. Ubbink and T. Odijk, Biophys. J. 68 (1995) 54; Europhys. Lett. 33 (1996) 353; N.V. Hud, K.H. Downing and R. Balhorn, Proc. Natl. Acad. Sci. USA 92 (1995) 3581.
[19] L.S. Lerman, Proc. Natl. Acad. Sci. USA 68 (1971) 1886; U.K. Laemmli, Proc. Natl. Acad. Sci. USA 72 (1975) 4288; Yu.M. Evdokimov et al. Nucl. Acid Res. 3 (1976) 2353; G.E. Plum, P.G. Arscott and V.A. Bloomfield, Biopolymers 30 (1990) 631; V.V. Vasilevskaya, A.R. Khokhlov, Y. Matsuzawa and K. Yoshikawa, J. Chem. Phys. 102 (1995) 6595.
[20] A.Yu. Grosberg, Biophysics 24 (1979) 30; A.Yu. Grosberg and A.R. Khokhlov, Adv. Polym. Sci. 41 (1981) 53.
[21] T. Garel and H. Orland, Europhys. Lett. 6 (1988) 307; 6 (1988) 597.
[22] C.D. Sfatos, A.M. Gutin and E.I. Shakhnovich, Phys. Rev. E 48 (1993) 465.
[23] V.S. Pande, A.Yu. Grosberg and T. Tanaka, Phys. Rev. E 51 (1995) 3381.
[24] E.G. Timoshenko, Yu.A. Kuznetsov and K.A. Dawson, Phys. Rev. E 54 (4) (1996) 4071.
[25] M. Mezard, G. Parisi and M. Virasoro, Spin Glass Theory and Beyond (World Scientific, Singapore, 1987).
[26] H.A. Scheraga, Pure Appl. Chem. 36 (1973) 1; N. Go and H. Taketomi, Proc. Natl. Acad. Sci. USA 75 (1978) 559; O. Ptitsyn and A. Finkelstein, Q. Rev. Biophys. 13 (1980) 339; P. Privalov, Adv. Protein Chem. 35 (1982) 1; O. Ptitsyn, J. Protein Chem. 6 (1987) 273; K.A. Dill, Biochemistry 24 (1985) 1501; 29 (1990) 7133; H. Frauenfelder, in: Structure and Dynamics of Nucleic acids, Proteins and Membranes, eds. E. Clementi and S. Chin (Plenum, New York, 1986); H. Frauenfelder, F. Parak and R. Young, Ann. Rev. Biophys. Biophys. Chem. 17 (1988) 451; M. Matsumoto, T. Sakaguchi, H. Kimura et al., J. Polym. Sci. B 30 (1992) 779; K. Minagawa, Y. Matsuzawa and K. Yoshikawa, A.R. Khokhlov and M. Doi, Biopolymers 34 (1994) 555.
[27] A.Yu. Grosberg and A.R. Khokhlov, Statistical Physics of Macromolecules (AIP, New York, 1994).
[28] D. Bratko and K.A. Dawson, J. Chem. Phys. 99 (1993) 5352.
[29] E.G. Timoshenko and K.A. Dawson, Phys. Rev. E 51 (1995) 492.
[30] E.G. Timoshenko and K.A. Dawson, unpublished.